Available online at www.sciencedirect.com

ScienceDirect

Mendeleev Commun., 2021, **31**, 804–806

Mendeleev Communications

Luminescent $[Cu_8I_8L_6]$ wheel and $[Cu_2I_2L_3]$ cage assembled from CuI and 3,6-bis(diphenylphosphino)pyridazine

Maxim I. Rogovoy, Mariana I. Rakhmanova, Taisiya S. Sukhikh and Alexander V. Artem'ev*

A. V. Nikolaev Institute of Inorganic Chemistry, Siberian Branch of the Russian Academy of Sciences, 630090 Novosibirsk, Russian Federation. E-mail: chemisufarm@yandex.ru

DOI: 10.1016/j.mencom.2021.11.011

The reaction of CuI and 3,6-bis(diphenylphosphino)pyridazine (dppz) in MeCN leads to the wheel-shaped complex $[Cu_8I_8(dppz)_6]$, assembled from four $[Cu_2I_2]$ units and six dppz ligands. This complex exhibits thermochromic luminescence with emission colors ranging from red (300 K) to deep red (77 K). When carried out in the presence of PPh_3, the reaction of CuI with dppz gives a non-emissive cage-like complex $[Cu_2I_2(dppz)_3]$, in which two CuI units are P,P′-bridged by three dppz ligands.

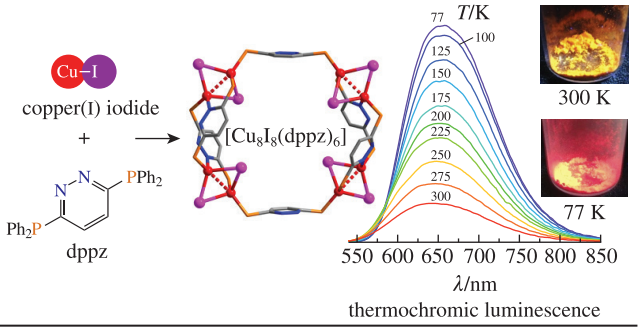

Keywords: copper(I) complexes, 3,6-bis(diphenylphosphino)pyridazine, wheel-shaped and cage-like complexes, thermochromic luminescence, crystal structure.

Currently, CuI-based coordination compounds are attracting considerable research interest due to their potential application in the production of light-emitting devices[1–3] and luminescent materials.[4–6] In particular, much attention is paid to the stimuli-responsive luminescence of these compounds (*e.g.*, thermo-, mechano-, rigido- and vapochromism).[7–10] All this, along with the rich coordination chemistry of cuprous iodide, a variety of organic ligands and various photophysical properties, makes CuI-based phosphors exciting objects for further research.

Among the known emissive complexes based on CuI, complexes with P-donor ligands, including various mono-[11] and polydentate phosphines,[12] are of great importance. Such CuI-phosphine complexes often exhibit bright thermally activated delayed fluorescence (TADF)[13] or phosphorescence[14] stemming from metal+halide-to-ligand charge transfer, ^{1}(M+X)LCT or ^{3}(M+X)LCT, respectively. Of particular interest are P,N-donor phosphines bearing azaheterocyclic fragments such as 2-pyridyl,[15] 2-pyrimidyl and 2-thiazolyl.[16,17] Using these P,N-ligands, many CuI-based complexes have been synthesized, showing remarkable emission properties. Nonetheless, among the above phosphines, pyridazyl-substituted ones remain the most unexplored in terms of the Cu^I coordination chemistry and luminescence,[18] although they represent a promising platform for designing CuI-assemblies. Despite several intriguing coinage metal complexes, little has been reported about their emission properties.[19,20]

In this work, we have investigated the reaction of CuI with 3,6-bis(diphenylphosphino)pyridazine (dppz) and synthesized the complex $[Cu_8I_8(dppz)_6]$ **1** with an intriguing wheel-shaped structure.† In the solid state, the latter exhibits red luminescence with a pronounced thermochromic behavior. In addition, the cage-like complex $[Cu_2I_2(dppz)_3]$ **2** has been obtained by reacting the above reactants in the presence of PPh_3.

Our experiments have shown that the interaction of dppz with CuI in a MeCN solution at room temperature leads to the formation of an octanuclear complex $[Cu_8I_8(dppz)_6]$ with a wheel-shaped structure, isolated as a solvate **1**·7MeCN in 85% yield. It is noteworthy that a change in the CuI/dppz ratio does not affect the result of the reaction. The complex is an orange microcrystalline powder, readily soluble in CH_2Cl_2 and almost insoluble in MeCN. According to single-crystal X-ray diffraction (scXRD) analysis, complex **1**·7MeCN crystallizes in the orthorhombic space group Fddd. Its molecular structure can be described as a wheel-shaped $[Cu_8I_8(dppz)_6]$ metallocycle containing four butterfly-shaped $[Cu_2I_2]$ fragments and six dppz molecules. In each $[Cu_2I_2]$ fragment, copper atoms are P,N-bridged by one dppz

† *Crystal data for* **1**·7MeCN. $C_{182}H_{153}Cu_8I_8N_{19}P_{12}$ (M = 4501.57), orthorhombic, space group *Fddd*, a = 23.867(5), b = 36.058(5) and c = 41.705(8) Å, V = 35891(11) Å^3, Z = 8, T = 150 K, d_{calc} = 1.620 g cm^{-3}. Total of 77367 reflections were measured, μ(MoKα) = 2.466 mm^{-1}, and 7395 independent reflections (R_{int} = 0.0945) were used in the further refinement. The refinement converged to wR_2 = 0.2590 and GOF = 1.044 for all independent reflections [R_1 = 0.0815 was calculated against F for 4367 observed reflections with $I > 2\sigma(I)$].

Crystal data for **2**·2Et$_2$O·MeCN·CH$_2$Cl$_2$. $C_{95}H_{91}Cl_2Cu_2I_2N_7O_2P_6$ (M = 2000.34), orthorhombic, space group $Pca2_1$, a = 27.0400(16), b = 13.0761(9) and c = 26.5092(13) Å, V = 9373.1(10) Å^3, Z = 4, T = 150 K, d_{calc} = 1.418 g cm^{-3}. Total of 39670 reflections were measured, μ(MoKα) = 1.322 mm^{-1}, and 14524 independent reflections (R_{int} = 0.0567) were used in the further refinement. The refinement converged to wR_2 = 0.1240 and GOF = 1.024 for all independent reflections [R_1 = 0.0481 was calculated against F for 11552 observed reflections with $I > 2\sigma(I)$]. Flack parameter = 0.29(2).

X-ray quality crystals of **1**·7MeCN were obtained by crystallization in MeCN in a U-shaped tube over 3–5 days. Single crystals of **2**·2Et$_2$O·MeCN·CH$_2$Cl$_2$ were crystallized by slow diffusion of Et$_2$O vapor into the CH$_2$Cl$_2$ solution. Diffraction data for the crystals of **1**·7MeCN and **2**·2Et$_2$O·MeCN·CH$_2$Cl$_2$ were obtained on an automated Bruker D8 Venture diffractometer with a CMOS PHOTON III detector and IμS 3.0 source [λ(MoKα) = 0.71073 Å, φ- and ω-scans]. Data collection, integration

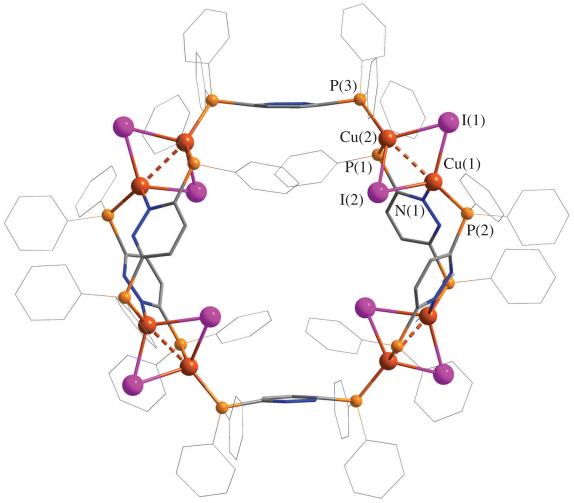

Figure 1 A wheel-shaped molecular structure of **1**·7MeCN. The solvent molecules and H atoms are omitted for clarity, and thin lines illustrate phenyl rings. Selected bond lengths (Å): I(1)–Cu(1) 2.599(2), I(1)–Cu(2) 2.680(2), I(2)–Cu(1) 2.7112(19), I(2)–Cu(2) 2.703(2), Cu(1)–Cu(2) 2.665(2), Cu(1)–P(2^i) 2.224(4), Cu(1)–N(1) 2.079(10), Cu(2)–P(1) 2.244(4), Cu(2)–P(3) 2.241(5). Selected bond angles (°): I(1)–Cu(1)–I(2) 110.56(7), P(2^i)–Cu(1)–I(1) 113.58(12), P(2^i)–Cu(1)–I(2) 102.75(11), N(1)–Cu(1)–I(1) 116.6(3), N(1)–Cu(1)–I(2) 101.5(3), N(1)–Cu(1)–P(2^i) 110.2(3), I(1)–Cu(2)–I(2) 108.39(6), P(1)–Cu(2)–I(1) 108.81(11), P(1)–Cu(2)–I(2) 102.07(12), P(3)–Cu(2)–I(1) 105.86(13), P(3)–Cu(2)–I(2) 108.85(14), P(3)–Cu(2)–P(1) 122.28(16). Symmetry code: (i) $-x + 3/4$, y, $-z + 3/4$.

ligand and P-monocoordinated by two other dppz molecules (Figure 1). Thus, Cu atoms have two coordination geometries: $\{CuP_2I_2\}$ and $\{CuPNI_2\}$. Both Cu(1) and Cu(2) have a four-coordinated tetrahedral environment (τ_4 = 0.91, τ_4' = 0.96),[24] completed by a short cuprophilic contact of 2.6635(3) Å (compare with the sum of the van der Waals radii of copper atoms equal to 2.80 Å). The $[Cu_8I_8(dppz)_6]$ rings contain voids (*ca.* 5 × 10 Å), which contain disordered MeCN molecules associated *via* weak contacts C–N···H–C_{Ph} and N–C···H–C_{Ph} (Figure S1).‡

We hypothesized that the studied reaction, when carried out in the presence of PPh_3 or other phosphines, would lead to CuI–dppz complexes bearing these phosphines as ancillary ligands. In contrast to our expectations, the reaction yields exclusively complex **2**, in which no coordinated PPh_3 was observed. PPh_3 likely mediates the reaction to form a CuI–PPh_3 adduct, which further interacts with the dppz ligand, leading to complex **2**. Under optimal conditions (CuI/dppz/Ph_3P = 2 : 3 : 10, CH_2Cl_2, room temperature), the isolated yield of complex **2** is 88%. Replacing PPh_3 with $(4\text{-}CF_3\text{-}C_6H_4)_3P$ and $(C_6F_5)_3P$ does not change the reaction outcome. Complex **2** is a microcrystalline powder insoluble in MeCN and slightly soluble in CH_2Cl_2. As shown by scXRD analysis, complex **2** crystallizes in the space group $Pca2_1$. Its molecule has a cage-like structure in which two CuI fragments are linked to the

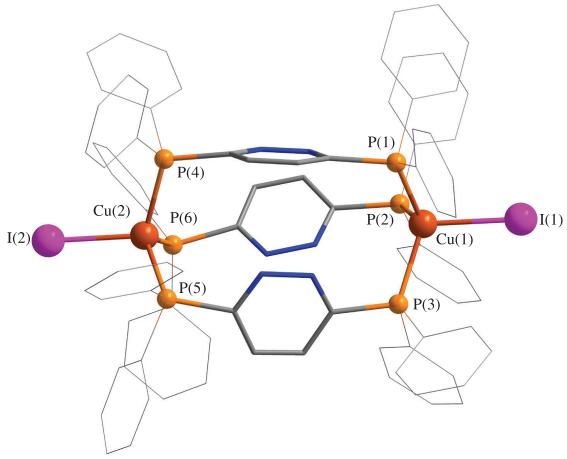

Figure 2 The metallocage structure $[Cu_2I_2(dppz)_3]$ in the crystals of complex **2**·$2Et_2O$·MeCN·CH_2Cl_2. H atoms are omitted for clarity, and thin lines illustrate phenyl rings. Selected bond lengths (Å): I(2)–Cu(2) 2.6121(15), Cu(2)–P(6) 2.281(3), I(1)–Cu(1) 2.6572(15), Cu(1)–P(3) 2.290(3), Cu(2)–P(4) 2.292(3), Cu(1)–P(2) 2.317(3), Cu(2)–P(5) 2.297(3), Cu(1)–P(1) 2.303(3). Selected bond angles (°): P(4)–Cu(2)–I(2) 109.22(9), P(3)–Cu(1)–I(1) 105.37(9), P(4)–Cu(2)–P(5) 111.51(11), P(3)–Cu(1)–P(2) 117.77(12), P(5)–Cu(2)–I(2) 106.55(9), P(3)–Cu(1)–P(1) 108.42(11), P(6)–Cu(2)–I(2) 103.05(9), P(2)–Cu(1)–I(1) 109.12(8), P(6)–Cu(2)–P(4) 112.94(12), P(1)–Cu(1)–I(1) 106.52(8), P(6)–Cu(2)–P(5) 112.97(11), P(1)–Cu(1)–P(2) 109.06(11).

P-atoms of three bridging dppz ligands (Figure 2). Each metal center adopts a tetrahedral environment $\{CuP_3I\}$ (τ_4 = 0.97), consisting of three P atoms from three dppz ligands (Cu–P distances = 2.28–2.31 Å) and one iodide anion (Cu–I distances = = 2.61–2.66 Å). The intramolecular Cu···Cu separation of *ca.* 7.5595(4) Å is too large for any cuprophilic interactions.

A freshly prepared solvate **1**·7MeCN partially loses solvate molecules during storage to form solvate **1**·4MeCN. The composition of the latter was confirmed by TGA data, which shows a slight decrease in weight at 20–80 °C due to the loss of the remaining MeCN molecules (Figure S3).‡ Complex **1** itself is stable up to 330 °C, after which a gradual weight loss is observed. Complex **2** demonstrates a multistep decomposition pattern, with three main steps appearing at 140–210, 240–275 and 300 °C. The FTIR spectra of complexes **1** and **2** almost coincide with the spectrum of the free dppz ligand (Figure S4).‡

We also have investigated the photophysical properties of complexes **1**·4MeCN and **2** in the solid-state. The UV-VIS absorption spectrum of compound **1**·4MeCN shows broad bands in the range of 200–400 nm, presumably due to the n–π* and π–π* intraligand transitions (Figure S5).‡ Moreover, a weak band is observed at *ca.* 390–580 nm, assignable to the (M+X)LCT transitions. Compound **2** exhibits almost the same absorption pattern in the high-energy region, but its (M+X)LCT band appears at 370–440 nm. The values of the optical band gap, estimated from the Tauc plot,[25] equal to 2.3 eV (**1**·4MeCN) and 2.9 eV (**2**), indicate the semiconducting nature of these complexes.

Under UV irradiation, a crystalline sample of complex **1**·4MeCN exhibits red photoluminescence (PL) in the form of a broad structureless band centered at 650 nm [Figure 3(*a*)], which does not change with variation of the excitation energy. The PL quantum yield at 300 K is 3% (λ_{ex} = 460 nm). The emission intensity increases significantly upon cooling to 77 K, and its color becomes deep red [Figure 3(*d*)]. This thermochromic behavior, visible to the naked eye, is in good agreement with the temperature-dependent PL spectra of complex **1**·4MeCN recorded in the range from 77 to 300 K [Figure 3(*b*)]. So, upon gradual cooling to 77 K, the intensity of the PL profile increases, and its maximum shifts to longer wavelengths by ~15 nm. The corresponding CIE chromaticity coordinates [Figure 3(*c*)] are also consistent

and determination of unit cell parameters were performed using APEX2, APEX3 and SAINT software, and absorption correction was applied based on the intensities of equivalent reflections using SADABS.[5] The structures were solved by a dual space algorithm (SHELXT[21]) and refined by the full-matrix least-squares technique (SHELXL[22]) in the anisotropic approximation (except hydrogen atoms). In the crystal of **1**·7MeCN, MeCN molecules are highly disordered, and the corresponding regions were removed from the intensity data following the OLEX2 Solvent Mask procedure (568 $\bar{e}$ in 4300 $Å^3$).[23] Positions of hydrogen atoms in organic ligands were calculated geometrically and refined in the riding model.

CCDC 2069364 and 2069366 contain the supplementary crystallographic data for this paper. These data can be obtained free of charge from The Cambridge Crystallographic Data Centre *via* http://www.ccdc.cam.ac.uk.

‡ For details, see Online Supplementary Materials.

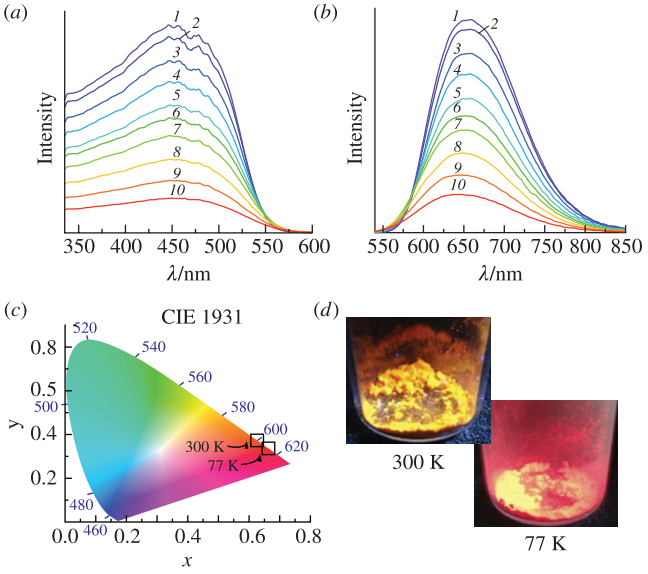

Figure 3 (*a*) Excitation (λ_{em} = 650 nm) and (*b*) emission (λ_{ex} = 450 nm) spectra of complex **1**·4MeCN at (*1*) 77, (*2*) 100, (*3*) 125, (*4*) 150, (*5*) 175, (*6*) 200, (*7*) 225, (*8*) 250, (*9*) 275 and (*10*) 300 K; (*c*) CIE diagram showing the thermochromic behavior of complex **1**·4MeCN [CIE coordinates: (0.6632, 0.33661) at 77 K and (0.62632, 0.37301) at 300 K]; (*d*) luminescent samples of complex **1**·4MeCN at 300 and 77 K.

with the visual PL color change. The PL decay of the compound under study at 300 K exhibits a monoexponential behavior with a lifetime of 1.2 μs. At 77 K, the emission lifetime increases by one order of magnitude and amounts to 27 μs. Considering the lifetime order and its significant increase upon cooling (1.2 μs → 27 μs), we can tentatively propose the TADF mechanism for the above complex. This assignment is indirectly confirmed by the fact that the $[Cu_2I_2]$ complexes, which are structurally similar to the $[Cu_2I_2]$ unit of complex **1**, generally display TADF of the (M+X)LCT type.[26] On the contrary, complex **2** has practically no apparent luminescence both at ambient temperature and at liquid nitrogen temperature.

In summary, the reaction of CuI with 3,6-bis(diphenylphosphino)pyridazine (dppz) has been investigated, and thus two Cu^I complexes have been synthesized. The molecule of the first complex is a structurally intriguing wheel $[Cu_8I_8(dppz)_6]$, assembled from four $[Cu_2I_2]$ units and six dppz ligands, while the second complex is composed of $[Cu_2I_2(dppz)_3]$ metallocage molecules, consisting of two CuI units, bridged by three dppz ligands *via* P atoms. Photophysical studies have shown that the wheel-shaped complex exhibits red luminescence (λ_{em} = 650 nm) at ambient temperature. Moreover, the luminescence has thermochromic nature, expressed as a bathochromic shift of the emission band by ~15 nm upon cooling from 300 to 77 K. The presented results contribute to the coordination chemistry of Cu^I and the development of stimuli-responsive CuI-based emitters.

This work was supported by the Russian Foundation for Basic Research (grant no. 20-33-90253) and the Ministry of Science and Higher Education of the Russian Federation (project no. 121031700321-3). The authors thank the Multi-Access Chemical Research Centre of SB RAS for spectral and analytical measurements.

Online Supplementary Materials

Supplementary data associated with this article can be found in the online version at doi: 10.1016/j.mencom.2021.11.011.

References

1 E. Cariati, E. Lucenti, C. Botta, U. Giovanella, D. Marinotto and S. Righetto, *Coord. Chem. Rev.*, 2016, **306**, 566.
2 W. Liu, Y. Fang and J. Li, *Adv. Funct. Mater.*, 2018, **28**, 1705593.
3 X. Hei and J. Li, *Chem. Sci.*, 2021, **12**, 3805.
4 B. Li, H.-T. Fan, S.-Q. Zang, H.-Y. Li and L.-Y. Wang, *Coord. Chem. Rev.*, 2018, **377**, 307.
5 J. Conesa-Egea, F. Zamora and P. Amo-Ochoa, *Coord. Chem. Rev.*, 2019, **381**, 65.
6 M. S. Deshmukh, A. Yadav, R. Pant and R. Boomishankar, *Inorg. Chem.*, 2015, **54**, 1337.
7 Y. Zhang, M. Schulz, M. Wächtler, M. Karnahl and B. Dietzek, *Coord. Chem. Rev.*, 2018, **356**, 127.
8 K. Tsuge, Y. Chishina, H. Hashiguchi, Y. Sasaki, M. Kato, S. Ishizaka and N. Kitamura, *Coord. Chem. Rev.*, 2016, **306**, 636.
9 P. C. Ford, E. Cariati and J. Bourassa, *Chem. Rev.*, 1999, **99**, 3625.
10 W. Liu, Y. Fang, G. Z. Wei, S. J. Teat, K. Xiong, Z. Hu, W. P. Lustig and J. Li, *J. Am. Chem. Soc.*, 2015, **137**, 9400.
11 H. Kitagawa, Y. Ozawa and K. Toriumi, *Chem. Commun.*, 2010, **46**, 6302.
12 J. Zhang, C. Duan, C. Han, H. Yang, Y. Wei and H. Xu, *Adv. Mater.*, 2016, **28**, 5975.
13 A. Schinabeck, M. J. Leitl and H. Yersin, *J. Phys. Chem. Lett.*, 2018, **9**, 2848.
14 Y.-L. Song, B.-J. Jiao, C.-M. Liu, X.-L. Peng, M.-M. Wang, Y. Yang, B. Zhang and C.-X. Du, *Inorg. Chem. Commun.*, 2020, **112**, 107689.
15 D. M. Zink, M. Bächle, T. Baumann, M. Nieger, M. Kühn, C. Wang, W. Klopper, U. Monkowius, T. Hofbeck, H. Yersin and S. Bräse, *Inorg. Chem.*, 2013, **52**, 2292.
16 T. Baumann, *Patent WO 2013/072508*, 2013.
17 J. M. Busch, D. M. Zink, P. Di Martino-Fumo, F. R. Rehak, P. Boden, S. Steiger, O. Fuhr, M. Nieger, W. Klopper, M. Gerhards and S. Bräse, *Dalton Trans.*, 2019, **48**, 15687.
18 H. Yersin, U. Monkowius, T. Fischer, T. Hofbeck, T. Baumann and T. Grab, *Patent WO 2010/149748*, 2010.
19 I. O. Koshevoy, L. Koskinen, E. S. Smirnova, M. Haukka, T. A. Pakkanen, A. S. Melnikov and S. P. Tunik, *Z. Anorg. Allg. Chem.*, 2010, **636**, 795.
20 V. J. Catalano, M. A. Malwitz, S. J. Horner and J. Vasquez, *Inorg. Chem.*, 2003, **42**, 2141.
21 G. M. Sheldrick, *Acta Crystallogr., Sect. A: Found. Adv.*, 2015, **71**, 3.
22 G. M. Sheldrick, *Acta Crystallogr., Sect. C: Struct. Chem.*, 2015, **71**, 3.
23 O. V. Dolomanov, L. J. Bourhis, R. J. Gildea, J. A. K. Howard and H. Puschmann, *J. Appl. Crystallogr.*, 2009, **42**, 339.
24 L. Yang, D. R. Powell and R. P. Houser, *Dalton Trans.*, 2007, 955.
25 J. Tauc, R. Grigorovici and A. Vancu, *Phys. Status Solidi*, 1966, **15**, 627.
26 D. Volz, A. F. Hirschbiel, D. M. Zink, J. Friedrichs, M. Nieger, T. Baumann, S. Bräse and C. Barner-Kowollik, *J. Mater. Chem. C*, 2014, **2**, 1457.

Received: 17th June 2021; Com. 21/6589